Journal of Applied Polymer Science

Biodegradable composites with improved barrier properties and transparency from the impregnation of PLA to bacterial cellulose membranes

Leire Urbina,[1] Itxaso Algar,[1] Clara García-Astrain,[1] Nagore Gabilondo,[1] Alba González,[2] MªAngeles Corcuera,[1] Arantxa Eceiza,[1] Aloña Retegi[1]

[1]Materials+Technologies Group, Department of Chemical and Environmental Engineering, University of the Basque Country, Europa Plaza 1, Donostia-San Sebastian, 20018, Spain

[2]POLYMAT, Department of Polymer Science and Technology, University of the Basque Country (UPV/EHU), P.O. Box 1072, Donostia/San Sebastián, 20080, Spain

Correspondence to: A. Retegi (E-mail: alona.retegui@ehu.eus)

ABSTRACT: Poly(lactic acid) (PLA) was impregnated in bacterial cellulose (BC) membranes. BC/PLA films were prepared by solvent casting and mechanical, optical and barrier properties, and biodegradation process were investigated. The transparency of processed films was higher than that of neat BC and increased with PLA content. Moreover, the incorporation of PLA to BC enhanced significantly the water vapor barrier properties of the BC membranes. The bionanocomposites contained a high percentage of cellulose due to the impregnation method that leads to the film with a BC content of 94%, which practically maintains the excellent mechanical properties of BC. However, when increasing the PLA content in the bionanocomposites the mechanical properties decreased slightly with respect to BC. Biodegradation under real soil conditions was determined indirectly through the study of the visual degradation and disintegration, demonstrating that the bionanocomposites were degraded faster than the neat PLA. The successful production of BC/PLA bionanocomposites suggested the possible application of them for active food packaging. © 2016 Wiley Periodicals, Inc. J. Appl. Polym. Sci. **2016**, *133*, 43669.

KEYWORDS: biodegradable; biopolymers and renewable polymers; biosynthesis of polymers; membranes; packaging

Received 27 November 2015; accepted 21 March 2016

DOI: 10.1002/app.43669

INTRODUCTION

In recent decades, the transformation of the lifestyle of our society has led to changing consumption habits, which are reflected in the waste generated in our homes. The saturation levels of our landfills are the result of the new culture of throwaway and excessive packaging of products. Therefore, our society must use the acquired knowledge, expertise, and innovation to create new biodegradable materials in accordance with the current legislation.[1] In this context, biopolymers, biodegradable packaging materials which are obtained from renewable resources, represent an alternative to petroleum derived plastics because their degradation process leads to non-toxic or non-environmentally harmful residues. However, their use in packaging is restricted due to the poor barrier, mechanical, and thermal properties. To overcome this drawbacks and as a promising alternative, a new class of materials called bio-nanocomposites have been considered. These materials exhibit enhanced barrier, mechanical, and thermal properties due to their nanometric size.

Poly(lactic acid) (PLA), a thermoplastic polymer derived from renewable resources, has been widely studied in this field since it presents some attractive characteristics such as renewability, transparency, biodegradability, and relatively low cost.[2] In fact, PLA can be processed combined with different types of nanoreinforcements or polymers to obtain composites for a variety of applications.[3,4] Nakagaito *et al.* produced microfibrillated cellulose (MFC)-reinforced poly(lactic acid) (PLA) nanocomposites and the study revealed that the modulus, strength, and strain at fracture increased linearly with the MFC content.[5] Nevertheless, the use of PLA for food packaging still presents some challenges. On the one hand, the thermal and mechanical properties of PLA are inferior to those of conventional petroleum-based polymers.[6] On the other hand, the incorporation of nanocelluloses into PLA matrices, which have hydrophobic nature, is not easy as the nanoparticles tend to form aggregations due to their hydrophilicity. For this reason, different processing methods have been reported to improve the interfacial compatibility

between these nanocellulosic substrates and the PLA, such us injection of aqueous suspension of cellulose nanofibrils (NFCs) in the melt PLA during the extrusion, electrospinning, or solution-casting.[2] There are several studies using solvent-casting method and have achieved a uniform dispersion of the reinforcement in the PLA matrix.[7–10]

Recently, bacterial cellulose (BC), a natural polymer synthesized by the fermentation process of bacteria belonging to genera *Gluconacetobacter, Rhizobium, Sarcina, Agrobacterium, Alcaligenes* among others, has been regarded as reinforcing element for biopolymers due to its interesting properties.[11] In fact, BC nanowhiskers have been used to develop coated systems with PLA by electrospinning.[12] BC presents excellent mechanical properties even at wet state, high water-holding capacity, moldability, crystallinity, and biocompatibility that make it very attractive for various fields of application such as food packaging, medicine or catalysis. Despite BC presents the same chemical structure as cellulose from plants, the 3D network-like structure formed by cellulose nanofibers during its biosynthesis derives in different conformation and its final physico-chemical properties.[13] However, the hydrophilic nature of BC membranes and the filling of the existing free volume by water molecules can cause a reduction of the barrier properties compared to conventional polymers. Although there are several studies in which PLA matrix has been used reinforced with various types of celluloses, such us natural fibers, cellulose nanocrystals or nanowhiskers,[14–16] to the best of our knowledge, no work was found that exploits the excellent mechanical properties of the whole bacterial cellulose membrane obtained during the biosynthesis[13] to develop BC/PLA systems. Moreover, the impregnation methodology proposed in this work counteracts the difficulties to obtain good dispersion of large amounts of nanofibers in the polymer matrix and the filling of the gaps between the nanofibers of the BC membrane by the PLA can lead to an improvement of the barrier properties. In this work, BC/PLA biodegradable bionanocomposites using different PLA loading percentages have been developed and the water vapor permeability (WVP), mechanical behavior, and biodegradability of the obtained bionanocomposites have been analyzed.

MATERIALS AND METHODS

Materials

Poly(lactic acid) (PLA 3051D, in pellets, molecular weight of 1.42×10^4 Da) was supplied by Nature Works LLC (Minnetonka, Minnesota, USA). Potassium hydroxide (KOH) was obtained by Panreac. Polyethylene glycol 8000 (PEG) was purchased from Aldrich (Spain). Chloroform was used as solvent.

Preparation of Bacterial Cellulose Membranes

Bacterial cellulose biosynthesis was carried out using commercial sugar cane and pineapple peel bought in a local supermarket as nutrients. It was obtained in the laboratory of the research group from *Gluconacetobacter medellinensis* bacterial strain whose cells, like all the cellulose producer bacteria, possess pores in their membrane for cellulose extrusion and secretion into the culture medium. Besides, the desired thickness of the BC membrane depends on the growing time. BC pellicles were incubated for 13 days at 28 °C in a static culture containing 13.0% (wt/vol) sugar and agricultural pineapple residues in water adjusting pH with acetic acid to 3.3 in a glass flask according to our previously developed procedure.[17] Then, BC membranes with a thickness of 0.5–0.7 cm and 9 cm of diameter were boiled in KOH (5 wt %) solution for 60 min at 120 °C in order to remove non-cellulosic compounds and then thoroughly washed under running water for 2 days until a complete neutralization. Then, KOH-treated BC membranes were suspended in distillated water and maintained until their use.

Preparation of BC/PLA-PEG Films

BC/PLA bionanocomposites were prepared by solvent casting method. After checking in several impregnation tests the poor compatibility between the hydrophobic PLA and hydrophilic BC, the interaction between BC and PLA was improved by the addition of a small amount of polyethylene glycol (PEG). The ratio of PLA-PEG was fixed to 9/1 (wt/wt). Solutions with different PLA-PEG concentrations in chloroform (1, 5, 10, and 15 wt %) were prepared and chloroform wet BC membranes were immersed in these solutions and maintained in a vacuum oven for 2 h at room temperature. Finally, films were dried under ambient conditions during 2 weeks via compression between Teflon plates in order to avoid the shrinkage of the films. Films with a thickness of ±0.06 mm were obtained. All samples were conditioned at 60 °C for 24 h and then kept in a desiccator before testing.

NMR Spectroscopy

The composition of the BC/PLA-PEG films was determined by carbon-13 nuclear magnetic resonance (^{13}C NMR spectroscopy). ^{13}C NMR solid-state spectra were performed using Bruker 400 WB Plus spectrometer. Spectra were collected using a 4 mm cross-polarization magic angle spining (CP-MAS) probe at a spinning of 10,000 Hz. CP/MAS ^{13}C NMR spectra of solid samples were recorded for 12 h using the standard pulse sequence at 100.6 MHz, a time domain of 2K, a spectral width of 29 kHz, a contact time of 1.5 ms and an inter-pulse delay of 5 s at 25 °C. To calculate the PLA molar percentage in the bionanocomposites, two peaks were taken as a reference to measure the relationship of the areas: the peak of the C_1 at $\delta \sim 105$ of cellulose and the peak of the methyl group of PLA.

$$\text{PLA molar } \% = \frac{\text{Peak area } CH_{3\,PLA}}{\text{Peak area } CH_{3\,PLA} + \text{Peak area } C_{1\,BC}} \times 100 \quad (1)$$

Then, the weight percent of PLA was calculated using the molar percentage and the molecular weight of the repeating units of both cellulose and PLA.

$$\text{PLA weight } \% = \frac{\text{PLA molar } \% \times MW_{\text{repeating unit}}}{\text{PLA molar } \% \times MW_{\text{repeating unit}} + \text{BC molar } \% \times MW_{\text{repeating unit}}} \times 100 \quad (2)$$

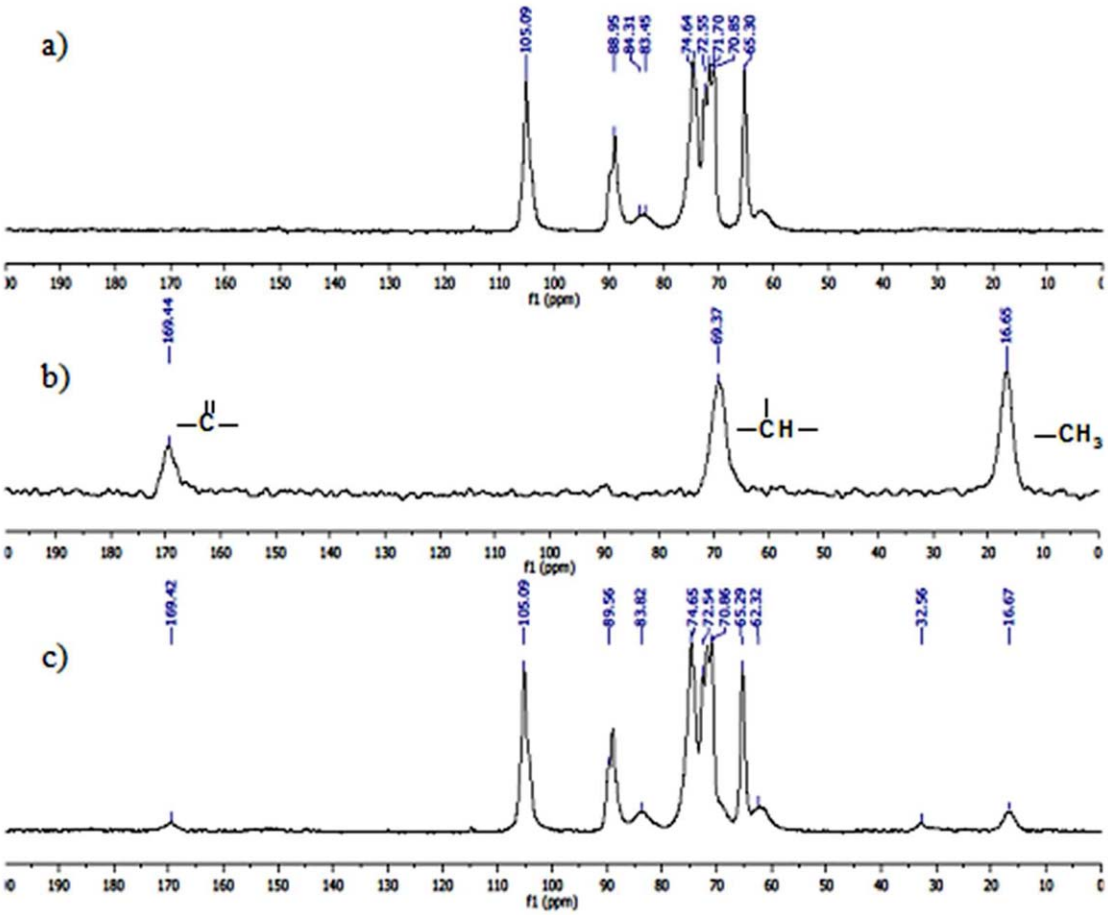

Figure 1. ^{13}C NMR spectra of (a) BC, (b) PLA-PEG blend, and (c) bionanocomposite from the solution of 1% PLA-PEG. [Color figure can be viewed in the online issue, which is available at wileyonlinelibrary.com.]

FTIR Spectroscopy

Attenuated Total Reflectance-Fourier Transform Infrared (ATR-FTIR) spectroscopy analysis was carried out to identify functional groups present in the samples and analyze interactions between PLA and BC on a Nexys Fourier transform infrared spectrophotometer from Nicolet in the range of 4000–400 cm^{-1}. All spectra were recorded with the accumulation of 32 scans with a resolution of 4 cm^{-1}.

Water Vapor Permeability (WVP)

The analysis of water vapor permeability was carried out with a Sartorius BP210D gravimetric cell. Taken into account the results obtained of time and weight gain, due to the water vapor that cross the film, water vapor transmission rate (WVTR) value could be calculated. This data is directly related with the water vapor permeability (WVP).

$$\mathrm{WVTR} = \frac{m \times l}{A(a_{in} - a_{out})} \tag{3}$$

$$\mathrm{WVP} = \frac{\mathrm{WVTR}}{p_v} \tag{4}$$

where m is the total mass of sample, l is the film thickness, A is the film area (2.54 cm^2), a_{in} and a_{out} are the relative humidity inside and outside the cell, and p_v is the saturation vapor pressure of water at test temperature. Three samples of each system were tested.

Mechanical Properties

Mechanical properties were measured using a 200 N load cell (Minimat 2000, Rheometrics Scientific) at room temperature. The samples were cut in 30 × 5 mm rectangular specimens. Initial grip separation was set at 22 mm, and crosshead rate was set at 2 mm/min following ASTM D1708 standard. At least eight samples were tested for each set of samples, being the average values reported.

Contact Angle Measurements

Contact Angle measurements were performed at 24 °C in a Video-Based Contact Angle System model OCA (optical contact angle). Contact Angle measurements were obtained by analyzing the shape of a distilled water drop after it was placed over the film for 20 s.

Biodegradability Tests

To ensure the biodegradability of the bionanocomposites, soil biodegradation tests were carried out under aerobic conditions at 60 °C (the minimum temperature for the degradation of the PLA) and at room temperature. To simulate real soil environment, the soil used in this study was a natural soil collected from the mountain of Basque country, in the ground surface

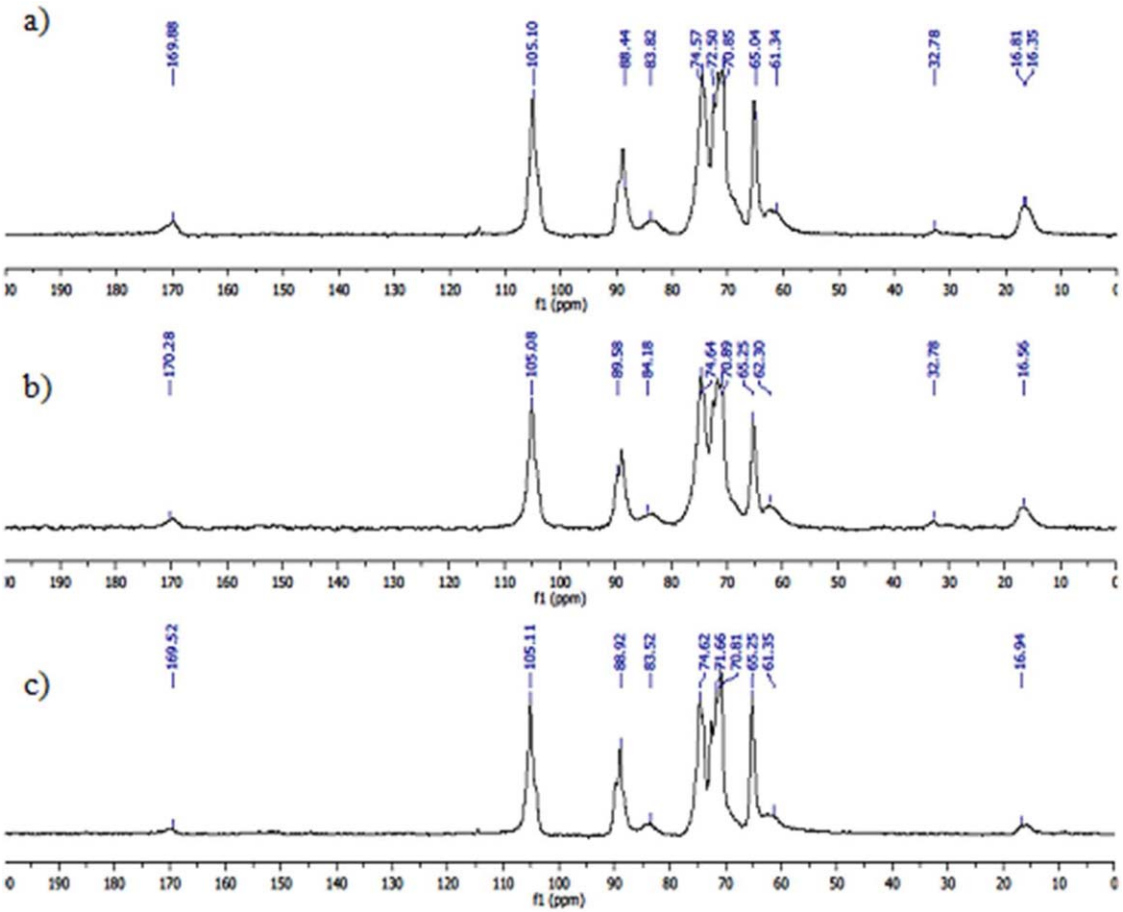

Figure 2. ^{13}C NMR spectra of the bionanocomposites from the solutions (a) 5% PLA-PEG, (b) 10% PLA-PEG, and (c) 15% PLA-PEG. [Color figure can be viewed in the online issue, which is available at wileyonlinelibrary.com.]

and the biodegradation was monitored using the processes of degradation and disintegration as strong indicators (but not as quantitative measures). Samples with different compositions were buried in the soil. Two specimens were tested for each system. After burying the samples, they were incubated and aerated every 4–5 days to ensure aerobic conditions. Water content was checked regularly, and water was added to ensure constant moisture content. For different time periods, sample extractions were performed in order to observe the state of them.

RESULTS AND DISCUSSION

Determination of BC/PLA Percentages in the Final Bionanocomposites

The CP/MAS ^{13}C NMR spectra recorded on the neat BC, PLA-PEG blend, and bionanocomposites in the dry state are shown in Figures 1 and 2. A typical CP/MAS ^{13}C NMR spectrum of isolated cellulose presents resonances in the shift ranges of $\delta \sim 102$–108 ppm (attributed to the C_1 of cellulose), $\delta \sim 80$–92 ppm (attributed to the C_4), and $\delta \sim 57$–67 ppm (attributed to the C_6) [see Figure 1(a)].[18] The carbons C_2, C_3, and C_5 of cellulose are reflected in the signal in the range of 70–80 ppm. After the impregnation process, there can be distinguish two chemical shifts located at 169 and 16 ppm in the bionanocomposites' spectra [Figures 1(c) and 2], assigned to the carbonyl group and methyl group ($–CH_3$) of PLA,[19] thus confirming the successful incorporation of PLA-PEG blend to the BC membrane. Moreover, comparing BC' and bionanocomposites' spectra it can be observed in the latest ones a widening of the cellulose peak at 69 ppm. This is ascribed to the peak overlap corresponding to the –CH– of the PLA. From these results, it has been possible to determine the actual composition of the synthesized films. Table I gathers the final composition of the bionanocomposites obtained from the starting solutions with different PLA-PEG concentrations. As it can be seen, the maximum PLA uptake was achieved with the concentration of 5% PLA-PEG and it decreases with increasing concentration. This occurred due to an increase of the viscosity in the solution, which hinders the incorporation of the PLA-PEG blend into the BC membrane network.

Table I. Final Composition of Synthesized Bionanocomposites According to the Starting Solutions

Starting solution	BC (%)	PLA (%)	System
1% PLA-PEG	94	6	BC94/PLA-PEG
5% PLA-PEG	89	11	BC89/PLA-PEG
10% PLA-PEG	91	9	BC91/PLA-PEG
15% PLA-PEG	96	4	BC96/PLA-PEG

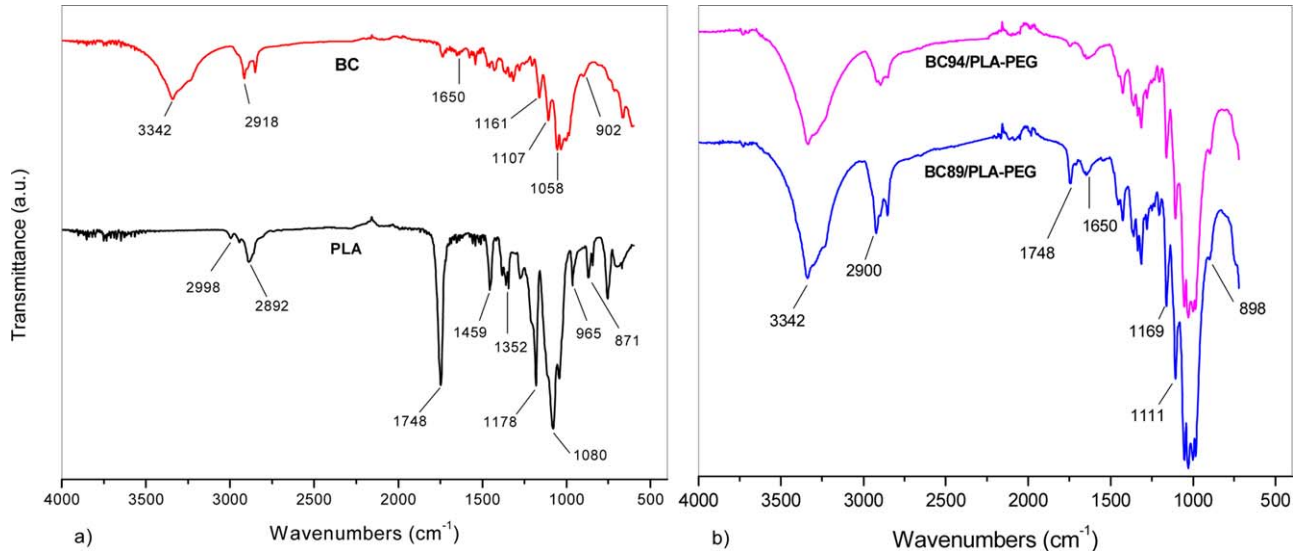

Figure 3. FTIR spectra of (a) PLA and BC; and (b) two of the bionanocomposites. [Color figure can be viewed in the online issue, which is available at wileyonlinelibrary.com.]

FTIR Characterization of the BC/PLA Bionanocomposites

FTIR analysis is commonly used to identify interactions between polymers in the composites. In Figure 3, the FTIR spectra of neat bacterial cellulose and PLA and two bionanocomposites are shown. BC and PLA peaks assignments and corresponding positions are given in the Table II. [17,20,21]

From the spectrum of BC it can be observed the bands located at around 3400–3300 cm^{-1} that correspond to O–H cellulose stretching and bending vibrations. The absorption bands at 2900–2880 cm^{-1} and 1460–1250 cm^{-1} are assigned to the CH and CH_2 stretching and bending vibrations, respectively. Besides, the bands at 1170–1050cm^{-1} are assigned to the vibrations of the C–O–C bond of the glycosidic bridges. The broad band at 902 cm^{-1} is characteristic of β-linked glucose based polymers. Finally, the band at around 1650 cm^{-1} is assigned to the water absorbed by the cellulose.

The PLA spectrum shows the stretching peak of the C = O at 1748 cm^{-1}. The peaks at 2995, 2998, 2892, 1459, and 1352 cm^{-1} are the asymmetric stretching, symmetric stretching, symmetric bending, and asymmetric bending of –CH–. The peaks at 1178 and 1080 cm^{-1} are attributed to the C–O stretching. In addition, the peaks of 965 and 871 cm^{-1} correspond to the stretching of the C–C single bond.

In the bionanocomposites' spectra, it can be observed many similarities with the BC spectrum due to the high cellulose content. With the incorporation of PLA the band located at 1750 cm^{-1} is observed but with low intensity. However, new peaks are not observed, what seems to confirm that chemical interactions between PLA and cellulose have not been produced. Other authors using cellulose nanofibers in a PLA matrix have reported that the absence of new characteristic peaks confirms that no new functional groups have been formed, suggesting only physical interactions between cellulose and the PLA/PEG.[21]

Film Opacity

In packaging applications, the transparency of the materials is an important characteristic. As it can be seen in Figure 4, whereas PLA-PEG film is fully transparent BC film is quite translucent and bionanocomposites are clearly more transparent. BC sheet can be considered as a three-dimensional network structure of nano-sized fibers with air interstices in between. The effect of the light diffraction at the interface between the cellulose fibers and these air interstices causes the opacity of the bacterial cellulose film.[22] BC bionanocomposites probably do not contain these interstices or gaps because they have been filled with the PLA-PEG during impregnation. This interaction has improved with the addition of the plasticizer. Besides, the

Table II. Peak Assignments for PLA and BC Spectra

PLA		Bacterial cellulose	
Assignment	Peak position (cm^{-1})	Assignment	Peak position (cm^{-1})
-CH- stretch	2892, 2995, 2998	O-H (stretch and bend)	3400-3300
-C=O- ester	1748	CH (stretch and bend)	2900-2880
-CH- deformation (symmetric and asymmetric bend)	1459, 1352	CH_2 (stretch and bend) Absorbed water	1460-1250 1650
-C-O- stretch	1178, 1080	C-O-C bond	1170-1050
-C-C- stretch	871, 965	β-linked glucose	902

Figure 4. Photographs of BC/PLA-PEG films. (a) BC; (b) BC94/PLA-PEG; (c) BC89/PLA-PEG; (d) BC91/PLA-PEG; (e) BC96/PLA-PEG; and (f) 1% PLA-PEG film. [Color figure can be viewed in the online issue, which is available at wileyonlinelibrary.com.]

transparency of the bacterial cellulose bionanocomposites has increased due to their smooth surface when incorporating the PLA to the membrane since this makes the light diffraction at the surface of the film more uniform.

Mechanical Behavior

The mechanical behavior of neat BC, PLA-PEG blend, and BC/PLA-PEG bionanocomposites was evaluated by tensile tests and their maximum stress (σ_{max}), Young's modulus (E), and elongation at break (ε_b) are gathered in Table III. As deduced from the table, pure BC film displayed a rigid and brittle behavior, with a high Young's modulus but low elongation at break. BC film shows high modulus value attributed to the uniform, continuous, and straight 3D nanoscale network of cellulosic elements oriented in-plane, characteristics that may have been improved by the chloroform and subsequent drying process via compression. In previous studies of our research group, high elastic modulus values for bacterial cellulose have also been obtained.[23,24] However, it have not been reached so high values of maximum elongation at break, so the initial vacuum and subsequent drying process might have contributed in increasing the strength of the films. In contrast, PLA-PEG film presented low modulus and maximum stress values compared to BC, although it turned out to be a very ductile material. The plasticizers usually enhance the flexibility and ductility of glassy polymers and also their processability. Hassouna *et al.* concluded that the ductility of PLA improved when it was plasticized with 20 wt % of low molecular weight poly(ethylene glycol) (PEG).[25] When incorporating PLA-PEG blend to BC, one of the bionanocomposites (BC94/PLA-PEG) kept the mechanical properties

Table III. Mechanical Properties, Water Vapor Transmission Rate (WVTR), and Contact Angle Measurements for Neat BC, PLA/PEG, and Nanocomposites

	E (GPa)	σ_{max} (MPa)	ε_b (%)	WVTR (g mm/m^2 day)	Contact angle (°)
BC	12.98±2.61	244.62±87.80	2.84±0.93	55.3 ±6.9	36.5±3.8
1% PLA-PEG film	0.60±0.17	49.92±14.00	>250	7.8 ± 0.2	33.3±2.5
BC94/PLA-PEG	12.63±4.99	331.24±149.64	3.18±0.90	46.0 ± 1.5	40.7±3.2
BC89/PLA-PEG	4.31±3.73	169.58±20.77	4.29±0.58	35.4 ± 0.1	41.3±4.2
BC91/PLA-PEG	6.37±3.59	105.60±74.67	2.41±0.90	29.6 ± 1.0	37.8±1.8
BC96/PLA-PEG	9.15±1.35	222.89±93.09	2.85±1.06	25.0 ± 0.9	48.2±5.8
PLA	-	-	-	-	77.6±2.1

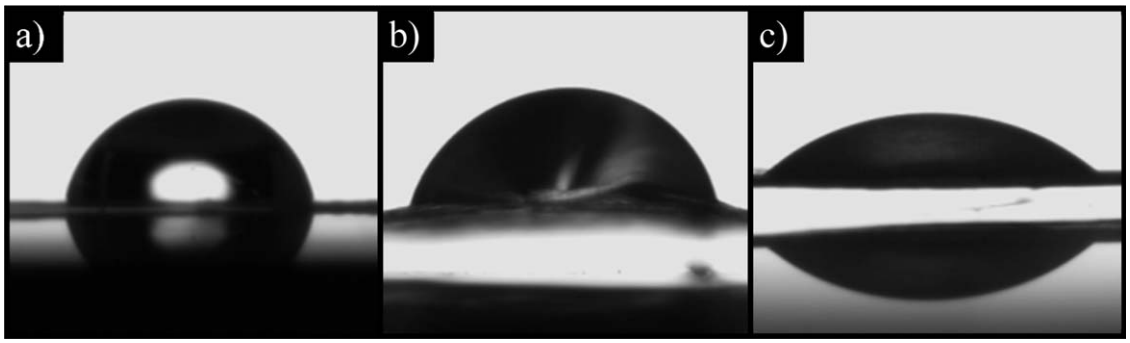

Figure 5. Contact angle photograms. (a) PLA, (b) BC96/PLA-PEG, and (c) BC.

of the BC due to the high cellulose content. However, the bionanocomposites with 91% and 89% of BC content experienced a reduction of Young's modulus and maximum stress compared to neat BC. This can be ascribed to the increase in the amount of PLA in the films, which reduces the strength and stiffness of the material. On the other hand, an evident decrease in the elongation at break of the BC/PLA-PEG bionanocomposites respect to the PLA-PEG blend was detected, thus confirming the brittle nature of these formulations. Generally, the addition of fibers causes a decrease of the elongation at break in the thermoplastic composites and this is affected by various factors such as the poor interaction between the reinforcement and the matrix, the dispersion of the fibers in the matrix, and the added volume fraction of reinforcement.[26] In this case, the high cellulose content (practically over 90% for all systems) contributes to the low elongation at break of these materials.

Barrier Properties of the Films

The water vapor barrier and wettability properties of the films were evaluated by measuring the water vapor transmission rates and the contact angle values for BC/PLA-PEG films.

The combination of the cellulose with outer layers of materials less sensitive to moisture to improve the barrier properties is a common trend and in this case, the effect of adding PLA to the BC matrix was analyzed. Table III gathers water vapor transmission rate values for the developed films. In the case of the PLA-PEG film the water vapor barrier level is in the level required in commercial packaging applications for dry food and pharmaceutics (0.1–10 g/m^2/day).[27] The BC film had low water vapor properties, since the network structure of nano-sized fibers with air interstices in between allows the water pass more easily through it. The addition of PLA-PEG blend enhanced the water vapor

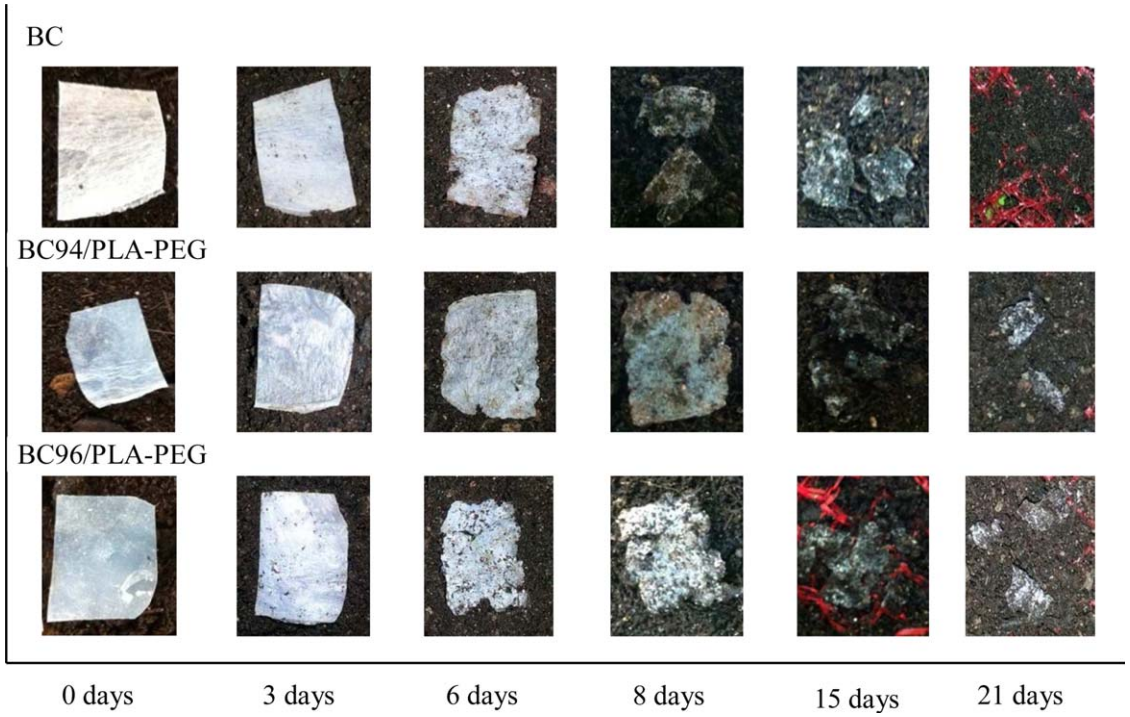

Figure 6. Photographs of neat BC and bionanocomposites taken at different incubation times at 60 °C. [Color figure can be viewed in the online issue, which is available at wileyonlinelibrary.com.]

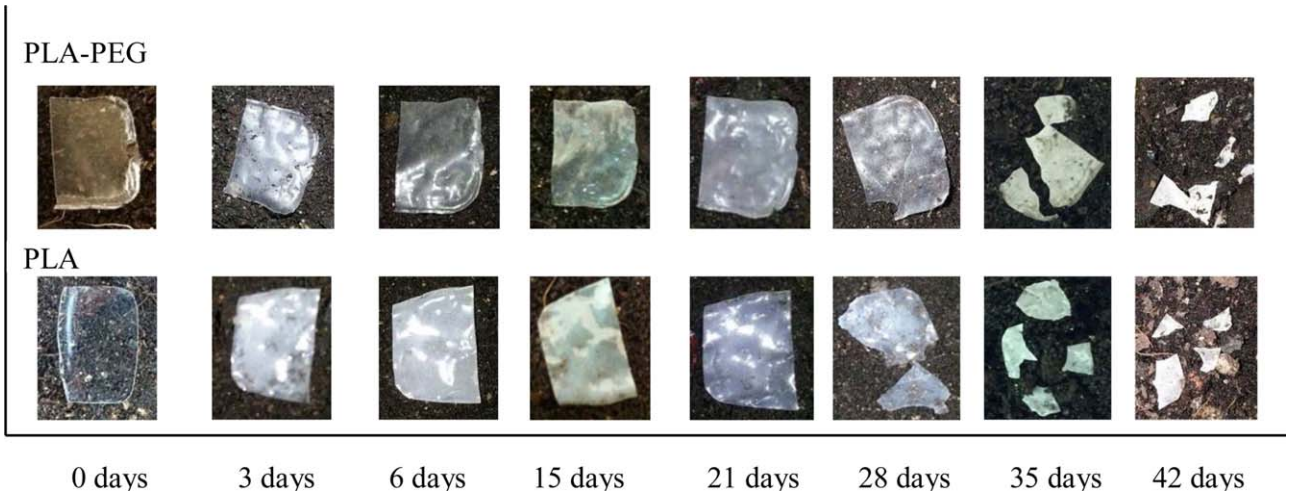

Figure 7. Photographs of neat PLA and PLA-PEG blend at different incubation times at 60 °C. [Color figure can be viewed in the online issue, which is available at wileyonlinelibrary.com.]

barrier properties of the BC film considerably. Here, the WVTR value was not found to decrease with the PLA-PEG content since the bionanocomposite with less PLA-PEG content achieved the lowest WVTR value by decreasing its value to 25 g/m^2/day. This probably occurred because the bionanocomposite obtained from the most concentrated solution (BC96/PLA-PEG) resulted in a layer of PLA in the BC membrane surface and it was not introduced into the nanofiber network due to the increased viscosity of the solution. Contact angle measurements were additionally carried out to investigate the effect of the incorporated PLA-PEG on the surface water affinity and results are gathered in Table III. Low contact angle values, ranging from 0° to 30°, are characteristic from highly hydrophilic surfaces such as glass or mica, while high contact angle values, between 70° and 90°, are observed for hydrophobic surfaces such as silicone or fluorocarbon polymers.[28] In this case the BC/PLA-PEG bionanocomposites turned to have more hydrophobic surfaces than the neat BC since it can be observed that the general tendency is an increase on the contact angle values of the bionanocomposites with respect to the neat BC. The increase of the contact angle can be ascribed to the fact that the PLA has been deposited in the films surface making them more hydrophobic. From Table III, it can be observed that the larger the contact angle is, the lower is the WVTR value, so the wettability properties of the samples correlate with the water vapor transmission rates. However, the PLA-PEG film shows a different behavior. As shown in Figure 5, PLA is an hydrophobic material, but when PEG was added to the PLA matrix the contact angle was reduced drastically respect to neat PLA despite the low plasticizer content. This can be ascribed to the hydrophilicity of PEG and also to the increase in roughness of the material

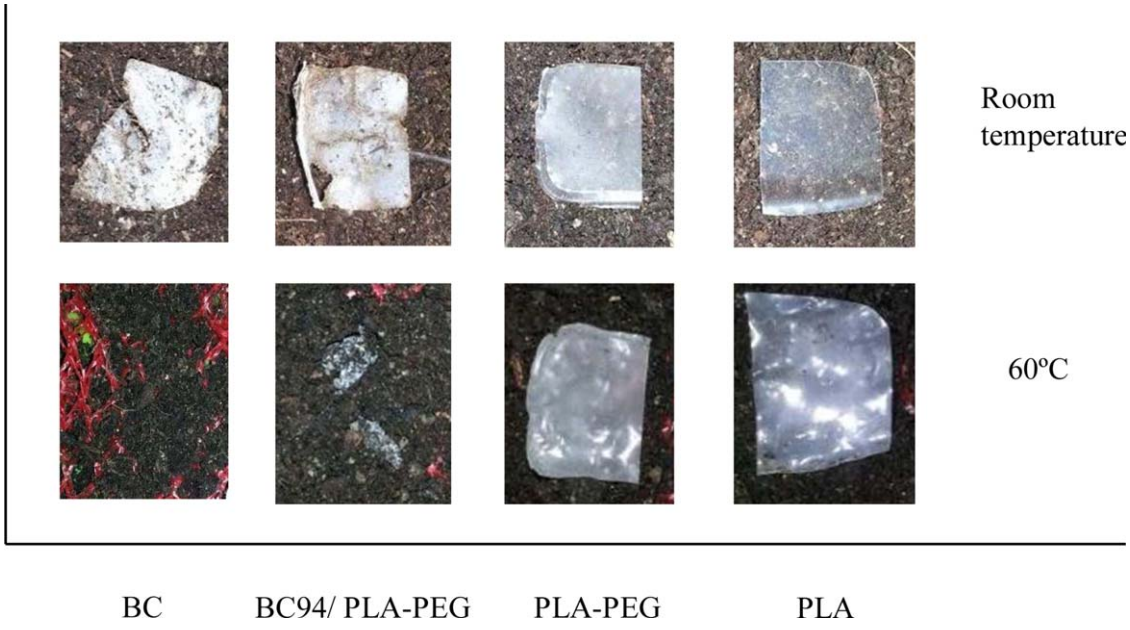

Figure 8. Photographs of neat BC, neat PLA, PLA-PEG blend, and one bionanocomposite at the 21st day at both 60 °C and room temperature. [Color figure can be viewed in the online issue, which is available at wileyonlinelibrary.com.]

when the PEG is added since it leads to a decrease in the contact angles in hydrophilic materials.[29]

Biodegradation Tests

In this work, disintegration of BC, PLA, PLA-PEG blend, and their bionanocomposites was carried out. Degradation tests were performed at both 60 °C and at room temperature in order to determine the effect of the temperature on the samples. The biodegradation of PLA is one of its most attractive properties for packaging applications and it takes place in two main stages. The first one is the hydrolytic degradation when the water starts to diffuse into the polymer. This is followed by the enzymatic degradation when the molecular weight is reduced and oligomers and lactic acid are formed due to the cleavage of ester linkages. These can be assimilated by microorganisms such as fungi and bacteria.[30] Regarding the degradation temperature of PLA, as the minimum temperature for crystallization is 60 °C, its degradation is not easy at lower temperatures and the temperature indicated by the international standards for biodegradation during composting is 58 °C.[31] In fact, studies have revealed that the hydrolysis phenomenon results faster at 58 °C, compared to 37 °C, and easy to be followed in a reasonable range of time.[32,33] Figures 6 and 7 show the samples taken out at different times of composting at 60 °C. The disintegration test (Figures 6 and 7) showed that neat PLA and PLA-PEG films were almost completely disintegrated after 42 days, while a different behavior was detected for BC/PLA-PEG bionanocomposites at different incubation times. It has been previously reported the influence of bio-based nanoparticles on the biodegradation in compost of PLA, such us microcrystalline cellulose, wood flour, wood pulp, and nanocrystalline cellulose.[6,34,35] Both bacterial cellulose and plant-derived one present two regions known as "crystalline cellulose" and "amorphous cellulose" which differ in the degree of orientation of the molecules. The first one is composed of highly oriented molecules while the second of less oriented ones. The physico-chemical characteristics of each substrate greatly affect the variation of the degradation capacity of cellulolytic microorganisms. These influential characteristics are the degree of crystallinity and polymerization of cellulose[36,37] although the crystallinity degree of cellulose is the most important structural parameter.[37] It has been previously reported that crystalline regions are more difficult to degrade.[38] BC shows much higher crystallinity compared to plant cellulose, which results in a relatively higher resistance to microorganism attacks. As cellulose is more easily degraded than PLA, and composites contain a considerable amount of BC, they were degraded in 21 days (Figure 6). The BC96/PLA-PEG film showed the best biodegradation behavior at 60 °C since it is the film with the highest BC content. Fragmentation and disintegration of the neat BC and synthesized bionanocomposites (Figure 6) started to be observed at the sixth day, while for PLA and PLA-PEG blend, (Figure 7) this was observed at the 28th day. As it can be observed, during the first 6 days for all the samples was detected some deformation and disintegration in addition to an increase of their opacity. These observations are signal that the hydrolytic degradation has started. The loss of their transparency is related to changes in the refractive index since during the degradation process there is a water absorption followed by the formation of low molecular weight compounds by the hydrolytic degradation.[39] Moreover, the crystallinity increases and holes are formed, factors that may contribute to the increase of the opacity.[40] On the other hand, the degradation process at room temperature resulted slower. Figure 8 shows the aspect of neat BC, neat PLA, PLA-PEG blend, and one bionanocomposites at the 21st day at both room temperature and 60 °C. It can be concluded that the temperature is an important variable in the process of decomposition of these materials due to the clear visual differences that present the samples. In contrast to the neat PLA and PLA-PEG blend samples, which show no signs of onset degradation, the bionanocomposites started to present disintegration at room temperature the 21st day.

CONCLUSIONS

In the present work, biodegradable BC/PLA-PEG bionanocomposites have been developed with interesting properties for packaging applications. To take advantage of the excellent mechanical properties of cellulose membrane obtained from its biosynthesis, PLA was incorporated to BC membrane by impregnation and solvent casting. The diffusion and wettability between the two components was improved by the plasticizer polyethylene glycol (PEG). The composition of bionanocomposites (BC content) was determined by ^{13}C NMR and it was observed that the PLA-PEG uptake decreased with solutions more concentrated than 5% PLA-PEG. This is the result of increasing the viscosity of the solution, which hinders the entry of the PLA-PEG blend into the BC network. While the sheet of neat BC is quite opaque, the synthesized films resulted more optically transparent. As expected, neat BC showed a high Young's modulus value, which makes it a rigid and brittle material. Due to the high cellulose content, the bionanocomposites showed high values of maximum stress and Young's modulus although the formulations with 89% and 91% of BC content presented a reduction of the mechanical properties compare to neat BC. The incorporation of PLA-PEG blend to the BC was found to significantly enhance the water vapor barrier properties of the BC film and increased the hydrophobicity of the surface of these films. Finally, biodegradation tests were carried out under real soil conditions in the laboratory at 60 °C and room temperature. The study of the degradation and disintegration of the materials was conducted by doing sample extractions at different time periods. The study revealed that the synthesized bionanocomposites were degraded in 21 days at 60 °C. Fragmentation of the neat BC and bionanocomposites started at the sixth day while for PLA and PLA-PEG blend this behavior was observed at the 28th day. On the other hand, at room temperature the degradation process was slower, as the fragmentation of the bionanocomposite films started at the 21st day. In conclusion, the methodology used for the incorporation of the PLA polymer to the BC membrane leads to obtain BC/PLA-PEG bionanocomposites with excellent barrier properties and biodegradable character that might be used in different fields of packaging.

ACKNOWLEDGMENTS

The authors thank for the financial support from the Basque Government in the frame of Saiotek S-PE13UN106, Grupos

Consolidados (IT-776-13), Foundation Domingo Martínez (2015-Área Materiales 2) and Spanish Ministry of Economy and Competitiveness (MINECO) (MAT2013-43076-R). We are also grateful to the research services (SGIker) of the UPV/EHU for allowing us to use the 'Macrobehaviour-Mesostructure-Nanotechnology' unit facilities. L.U. wishes to acknowledge the Basque Government (Ayudas para la Formación de Personal Investigador no doctor) for its PhD grant PIF PRE_2015_2_0009.

REFERENCES

1. Tang, X.; Kumar, P.; Alavi, S.; Sandeep, K. *Crit. Rev. Food. Sci. Nutr.* **2012**, *52*, 426.
2. Raquez, J. M.; Habibi, Y.; Murariu, M.; Dubois, P. *Prog. Polym. Sci.* **2013**, *38*, 1504.
3. Arrieta, M.; López, J.; Hernández, A.; Rayón, E. *Eur. Polym. J.* **2014**, *50*, 255.
4. Mi, H. Y.; Salick, M.; Jing, X.; Jacques, B.; Crone, W.; Peng, X. F.; Turng, L. S. *Mater. Sci. Eng.* **2013**, *33*, 4767.
5. Nakagaito, A. N.; Fujimura, A.; Sakai, T.; Hama, Y.; Yano, H. *Compos. Sci. Technol.* **2009**, *69*, 1293.
6. Fortunati, E.; Armentano, I.; Iannoni, A.; Barbale, M.; Zaccheo, S.; Kenny, J. M. *J. Appl. Polym. Sci.* **2012**, *124*, 87.
7. Li, Z. Q.; Zhou, X. D.; Pei, C. H. *Polym. Plast. Technol. Eng.* **2010**, *49*, 141.
8. Lin, N.; Huang, J.; Chang, P. R.; Feng, J.; Yu, J. *Carbohydr. Polym.* **2011**, *83*, 1834.
9. Tingaut, P.; Zimmermann, T.; Lopez-Suevos, F. *Biomacromolecules* **2009**, *11*, 454.
10. Pei, A.; Zhou, Q.; Berglund, L. A. *Compos. Sci. Technol.* **2010**, *70*, 815.
11. Ifuku, S.; Nogi, M.; Abe, K.; Handa, K.; Nakatsubo, F.; Yano, H. *Biomacromolecules* **2007**, *8*, 1973.
12. Martínez-Sanz, M.; Lopez-Rubio, A.; Lagaron, J. M. *Carbohydr. Polym.* **2013**, *98*, 1072.
13. Carreño, L. D.; Caicedo, L. A.; Martínez, C. A. *Ing. Cienc.* **2012**, *8*, 16, 307.
14. Bajpai, P. K.; Singh, I.; Madaan, J. *Wear* **2013**, *297*, 829.
15. Shi, Q.; Zhou, C.; Yue, Y.; Guo, W.; Wu, Y.; Wu, Q. *Carbohydr. Polym.* **2012**, *90*, 301.
16. Espino-Pérez, E.; Bras, J.; Ducruet, V.; Guinault, A.; Dufresne, A.; Domenek, A. *Eur. Polym. J.* **2013**, *49*, 3144.
17. Algar, I.; Fernandes, S. C.; Mondragon, G.; Castro, C.; Gabilondo, N.; Retegi, A.; Eceiza, A. *J. Appl. Polym. Sci.* **2014**, *132*, DOI: 10.1002/app.41237.
18. Foston, M. *Curr. Opin. Biotechnol.* **2014**, *27*, 176.
19. Hamad, W. Y.; Miao, C. U.S. Pat. 20,110,196,094 A1 (**2011**).
20. Kaya, M.; Odabasi, M.; Mujtaba, M.; Sen, M.; Bulut, E.; Akyuz, B. *Mater. Sci. Eng. C. Mater. Biol. Appl.* **2016**, *62*, 144.
21. Qu, P.; Gao, Y.; Wu, G. F.; Zhang, L. P. *Bioresources* **2010**, *5*, 1811.
22. Ummartyotin, S.; Juntaro, J.; Sain, M.; Manuspiya, H. *Ind. Crops. Prod.* **2012**, *35*, 92.
23. Retegi, A.; Gabilondo, N.; Peña, C.; Zuluaga, R.; Castro, C.; Gañan, P.; de la Caba, K.; Mondragon, I. *Cellulose* **2010**, *17*, 661.
24. Retegi, A.; Algar, I.; Martin, L.; Altuna, F.; Stefani, P.; Zuluaga, R.; Gañan, P.; Mondragon, I. *Cellulose* **2012**, *19*, 103.
25. Hassouna, F.; Raquez, J. M.; Addiego, F.; Dubois, P.; Toniazzo, V.; Ruch, D. *Eur. Polym. J.* **2011**, *47*, 2134.
26. Colom, X.; Carrasco, F.; Pages, P.; Canavate, J. *Compos. Sci. Technol.* **2003**, *63*, 161.
27. Vaha-Nissi, M.; Harlin, A.; Salomäki, M.; Areva, S.; Korhonen, J. T.; Karppinen, M. *Appl. Surf. Sci.* **2011**, *257*, 9451.
28. Gilliland, J. W.; Yokoyama, K.; Yip, W. T. *J. Phys. Chem. B* **2005**, *109*, 4816.
29. Chau, T. T.; Bruckard, W. J.; Koh, P. T. L.; Nguyen, A. V. *Adv. Colloid Interface Sci.* **2009**, *150*, 106.
30. Armentano, I.; Bitinis, N.; Fortunati, E.; Mattioli, S.; Rescignano, N.; Verdejo, R.; Lopez-Manchado, M. A.; Kenny, J. M. *Prog. Polym. Sci.* **2013**, *38*, 1720.
31. Gorrasi, G.; Pantani, R. *Polym. Degrad. Stab.* **2013**, *98*, 1006.
32. Höglund, A.; Hakkarainen, M.; Albertsson, A. C. *Biomacromolecules* **2010**, *11*, 277.
33. Höglund, A.; Odelius, K.; Albertsson, A. C. *ACS Appl. Mater. Interfaces* **2012**, *4*, 2788.
34. Fortunati, E.; Puglia, D.; Kenny, J. M.; Ul Haque, M.; Minhaz, Pracella, M. *Polym. Degrad. Stabil.* **2013**, *98*, 2742.
35. Bitinis, N.; Fortunati, E.; Verdejo, R.; Bras, J.; Kenny, J. M.; Torre, L.; López-Manchado, M. A. *Carbohydr. Polym.* **2013**, *96*, 621.
36. Amano, Y.; Nozaki, K.; Araki, T.; Shibasaki, H.; Kuga, S.; Kanda, T. *Cellulose* **2001**, *8*, 267.
37. Hall, M.; Bansal, P.; Lee, J. H.; Realff, M. J.; Bommarius, A. S. *FEBS J.* **2010**, *277*, 1571.
38. Alvarez, V. A.; Ruseckaite, R. A.; Vazquez, A. *Polym. Degrad. Stab.* **2006**, *91*, 3156.
39. Fukushima, K.; Abbate, C.; Tabuani, D.; Gennari, M.; Camino, G. *Polym. Degrad. Stabil.* **2009**, *94*, 1646.
40. Paul, M. A.; Delcourt, C.; Alexandre, M.; Degee, P.; Monteverde, F.; Dubois, P. *Polym. Degrad. Stabil.* **2005**, *87*, 535.